

Homoleptic Ruthenium Complex Bearing Dissymmetrical 4-Carboxy-4'-pyrrolo-2,2'-bipyridine for Efficient Sensitization of TiO₂ in Solar Cells

Arnald Grabulosa,[†] Marc Beley,^{†,‡} Philippe C. Gros,^{*,†} Silvia Cazzanti,[§] Stefano Caramori,^{*,§} and Carlo A. Bignozzi[§]

[†]*SRSMC, Nancy Université, CNRS, Faculté des Sciences, Boulevard des Aiguillettes, F-54506 Vandoeuvre-Lès-Nancy, France,* [‡]*Université Paul Verlaine, 57012 Metz, France,* and [§]*Chemistry Department, University of Ferrara, Via Luigi Borsari 46, 44100 Ferrara, Italy*

Received May 12, 2009

An easily accessible homoleptic complex [Ru(L3)]²⁺ containing a dissymmetrical bipyridine (L3) substituted by a pyrrole and a carboxylic group has been evaluated in a dye-sensitized solar cell. The new dye displayed extended absorption domain, high absorbance, and a promising 65% IPCE value. Higher scores were reached using a cobalt–iron mediator instead of the usual LiI/I₂ couple for regeneration of the Ru^{II} state. Transient absorption spectroscopy was used to explain the mediator effect.

Introduction

Dye-sensitized solar cells (DSCs) are efficient sunlight to electricity converters recognized as low-cost alternatives to silicon-based semiconductors.^{1–10} A critical component of these devices is the dye, which is usually a ruthenium-based complex linked via electron-withdrawing groups to nanoporous TiO₂ electrode. Its dual role is to ensure efficient harvesting of photons from sunlight and subsequent electron injection into the TiO₂ conduction band upon excitation of the central metal. An electron transport mediator is then used to regenerate the oxidized dye allowing the charge transport across the liquid phase in the solar cell. The central role played by the sensitizing dye has motivated modifications of the ligands around the metal to improve light harvesting (absorption domain, molar extinction coefficients). The trisheteroleptic RuL(dcbpy)(NCS)₂ complexes (L = bipyridine, dcbpy = 4,4'-dicarboxy-2,2'-bipyridine) have

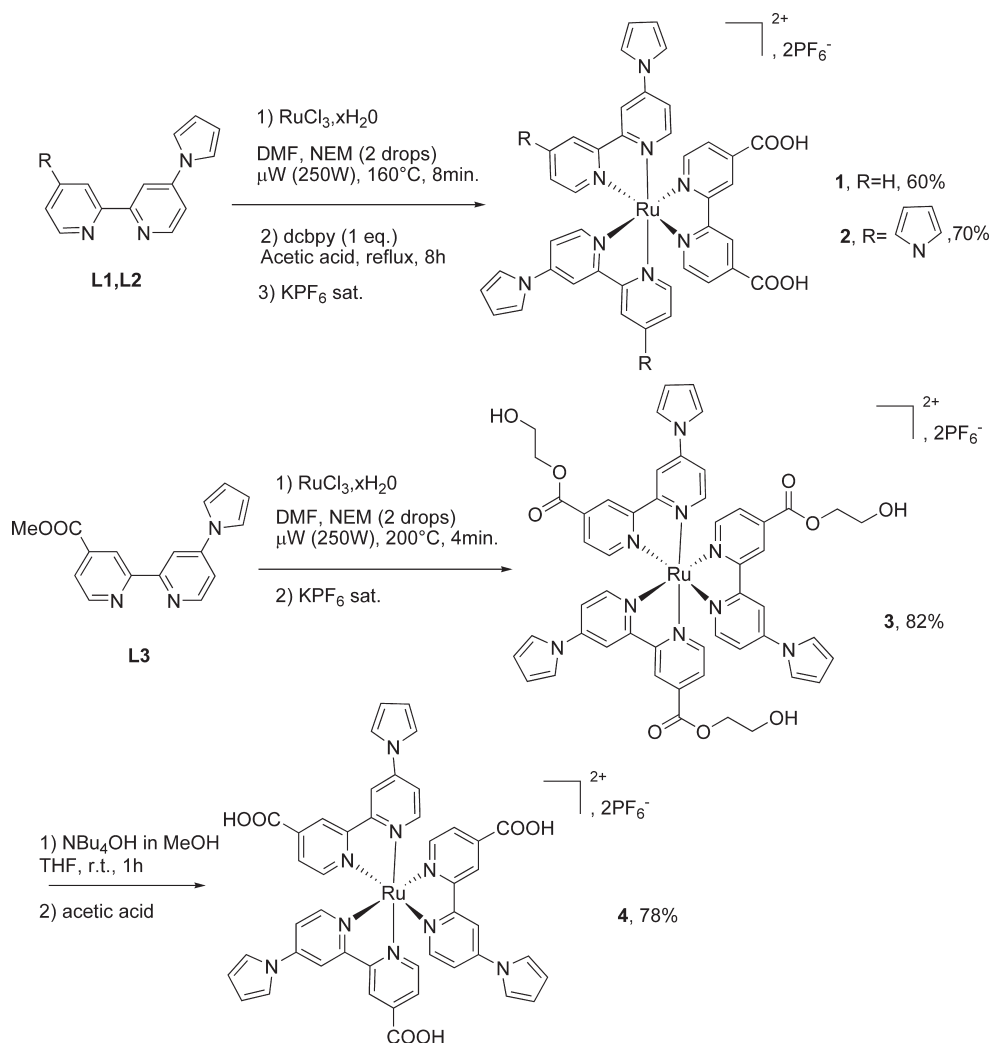
been widely studied. This family of complexes was reported to absorb light within a wide domain with high molar extinction coefficients,^{11–14} the most popular being N3 (Ru(dcbpy)₂(NCS)₂)^{15,16} and N719 which is obtained by deprotonation of one dcbpy in N3.¹⁷ Although the NCS groups greatly contribute to absorption domain widening by an additional electronic transition process, they also exhibit instability when the dye is in its oxidized form. They have been reported to be turned into cyano groups thus leading to dramatic alteration of performance and long-term stability.^{18,19} Thus approaches using bisheteroleptic [RuL₂(dcbpy)]²⁺ complexes remain of interest in the quest for stable and efficient dyes.

*To whom correspondence should be addressed. E-mail: philippe.gros@sor.uhp-nancy.fr (P.C.G.); cte@unife.it (S.C.).

- (1) Juris, A.; Balzani, V.; Barigelletti, F.; Campagna, S.; Belser, P.; Zelewsky, A. v. *Coord. Chem. Rev.* **1988**, *84*, 85–277.
- (2) O'Regan, B.; Grätzel, M. *Nature* **1991**, *353*, 737–740.
- (3) Hagfeldt, A.; Grätzel, M. *Chem. Rev.* **1995**, *95*, 49–68.
- (4) Argazzi, R.; Bignozzi, C. A.; Hasselmann, G. M.; Meyer, G. J. *Inorg. Chem.* **1998**, *27*, 4533–4537.
- (5) Curtright, A. E.; McCusker, J. K. *Inorg. Chem.* **1999**, *35*, 7032–7041.
- (6) Schulze, X.; Serin, J.; Adronov, A.; Fréchet, J. M. J. *Chem. Commun.* **2001**, 1160–1161.
- (7) Polson, M. I. J.; Taylor, N. J.; Hanan, G. S. *Chem. Commun.* **2002**, 1356–1357.
- (8) Wang, P.; Klein, C.; Humphry-Baker, R.; Zakeeruddin, S. M.; Grätzel, M. *J. Am. Chem. Soc.* **2005**, *127*, 808–809.
- (9) Li, S.-L.; Jiang, K.-J.; Shao, K.-F.; Yang, L.-M. *Chem. Commun.* **2006**, *26*, 2792–2794.
- (10) Robertson, N. *Angew. Chem., Int. Ed.* **2006**, *45*, 2338–2345.

- (11) Nazeeruddin, M. K.; Zakeeruddin, S.; Lagref, J.-J.; Liska, P.; Comte, P.; Barolo, C.; Viscardi, G.; Schenk, K.; Graetzel, M. *Coord. Chem. Rev.* **2004**, *248*, 1317–1328.
- (12) Wang, P.; Zakeeruddin, S. M.; Moser, J. E.; Humphry-Baker, R.; Comte, P.; Aranyos, V.; Hagfeldt, A.; Nazeeruddin, M. K.; Grätzel, M. *Adv. Mater.* **2004**, *16*, 1806–1811.
- (13) Nazeeruddin, M. K.; Wang, Q.; Cevey, L.; Aranyos, V.; Liska, P.; Figgemeier, E.; Klein, C.; Hirata, N.; Koops, S.; Haque, S. A.; Durrant, J. R.; Hagfeldt, A.; Lever, A. B. P.; Grätzel, M. *Inorg. Chem.* **2006**, *45*, 787–797.
- (14) Ito, S.; Ha, N.-L. C.; Rothenberger, G.; Liska, P.; Comte, P.; Zakeeruddin, S. M.; Pechy, P.; Nazeeruddin, M. K.; Grätzel, M. *Chem. Commun.* **2006**, 4004–4006.
- (15) Benko, G.; Kallioinen, J.; Korppi-Tommola, J. E. I.; Yartsev, A. P.; Sundstrom, V. *J. Am. Chem. Soc.* **2002**, *124*, 489–493.
- (16) Grätzel, M. *J. Photochem. Photobiol., A* **2004**, *164*, 3–14.
- (17) Nazeeruddin, M. K.; Kay, A.; Rodicio, I.; Humphry-Baker, R.; Mueller, E.; Liska, P.; Vlachopoulos, N.; Graetzel, M. *J. Am. Chem. Soc.* **1993**, *115*, 6382–6390.
- (18) Cecchet, F.; Gioacchini, A. M.; Marcaccio, M.; Paolucci, F.; Roffia, S.; Alebbi, M.; Bignozzi, C. A. *J. Phys. Chem. B* **2002**, *106*, 3926–3932.
- (19) Kohle, O.; Grätzel, M.; Meyer, A. F.; Meyer, T. B. *Adv. Mater.* **1997**, *9*, 904–906.

Scheme 1. Preparation of Complexes Studied in This Work



In this context, promising complexes **1** and **2** (Scheme 1) have been obtained from N-pyrrolo-bipyridine ligands. An efficient light-harvesting ability was observed and IPCE values up to 80% were measured.²⁰ Moreover, we have shown that the pyrrole moiety could be copolymerized with EDOP (3,4-ethylenedioxy-pyrrole) molecules giving access to new solid-state solar cells, the hole transporter being the polymer (PEDOP).²¹

However, a common drawback to the bishetero- and trisheteroleptic approach is the multistep reaction pathway needed for sequential introduction of the appropriate ligands around the metal often implying selectivity concerns and separations by size-exclusion chromatography. At first glance, homoleptic complexes appear more attractive by offering a straightforward access to dyes from adequately designed ligands. From our previous works on pyrrole-based bipyridine, we decided to investigate the properties of the homoleptic complex **4** (Scheme 1) containing a bipyridine bearing the electron-releasing pyrrole group on one ring and the electron-withdrawing carboxylic group on the other one.

In addition to simplified synthetic procedure, the presence of three anchoring carboxylic groups instead of two in **1** and **2** could improve the chemisorption on TiO_2 and subsequent charge injection into the conduction band.

Herein, we report on the characterization (UV-vis, electrochemistry) and photoelectrochemical performance of dye **4** in nanocrystalline TiO_2 solar cells and comparison of its properties with the bisheteroleptic pyrrole-based complexes.

Experimental Section

^1H and ^{13}C NMR have been recorded on AC200, AC250 or DRX400 Bruker spectrometers. Microwave experiments have been performed on a CEM Discover device fitted with infrared probe temperature control. Electrospray mass spectra have been recorded on an Agilent MSD using CH_3CN as solvent. The electrochemical measurements were performed with a PST006 analytical potentiostat using a conventional single compartment three-electrode cell. The reference electrode was the potassium chloride calomel electrode (SCE), the working electrode was a 10 mm Pt wire and the counter-electrode a 1 cm^2 vitreous carbon disk. The supported electrolyte was LiClO_4 0.1 M in CH_3CN and the solutions were purged with argon before each measurement. A 0.5 mM solution of the studied compound was generally used. All potentials are quoted versus SCE; in these conditions, the

(20) Martineau, D.; Beley, M.; Gros, P. C.; Cazzanti, S.; Caramori, S.; Bignozzi, C. A. *Inorg. Chem.* **2007**, *46*, 2272–2277.

(21) Caramori, S.; Cazzanti, S.; Marchini, L.; Argazzi, R.; Bignozzi, C. A.; Martineau, D.; Gros, P. C.; Beley, M. *Inorg. Chim. Acta* **2008**, *361*, 627–634.

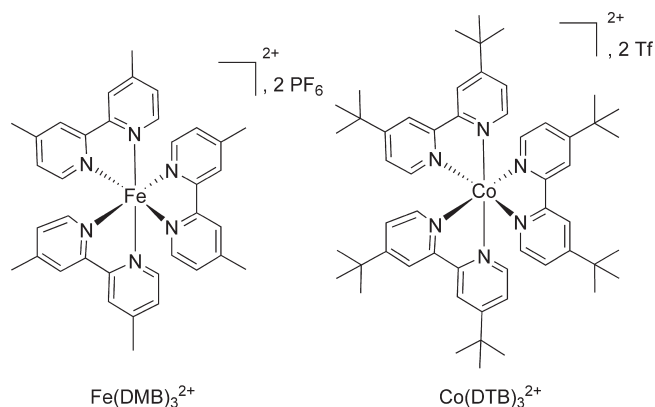
redox potential of Fc^+/Fc was found at 0.33 V. In all the experiments, the scan rate was 100 mV/s. Absorption UV–vis electronic spectra have been recorded on a Varian Cary E spectrometer and emission UV–vis electronic spectra on a SLM Aminco-Bowman Series 2 apparatus using a (1 cm \times 1 cm) quartz cell in deoxygenated solutions ($\text{OD} < 0.05$). Excited state lifetimes have been obtained by nanosecond transient absorption in acetonitrile as solvent by excitation at 355 nm of a laser Continuum Surelite II Q-switched Nd:YAG (fwhm = 7 ns, 8 Hz) laser. The probe beam, orthogonal to the excitation pulse, generated by a pulsed Xe lamp was focalized on an Acton Spectra Pro 2300i triple grating monochromator (5 nm band-pass) and detected with an Hamamatsu R 3896 photomultiplier. Oscillographic traces were acquired on a Lecroy 600 MHz oscilloscope and transferred to a personal computer by means of a custom-made labview program. Focalisation was realized by an Applied Photophysics monochromator. IPCE measurements were performed by illumination of the cell using an Osram 150 W xenon lamp coupled to an Applied Photophysics monochromator. The irradiated surface was 0.5 cm². Photocurrents were measured under short circuit conditions by a digital Agilent 34410A multimeter. Incident irradiance was measured with a 1 cm² Centronic OSD100–7Q calibrated silicon photodiode. J – V curves were recorded under both AM 1.5 G and monochromatic illumination by linearly sweeping the potential with a scan speed of 10 mV/s using an EcoChemie PGSTAT 302/N potentiostat.

TiO₂ Electrode Preparation.²² TiO₂ colloidal paste was prepared by hydrolysis of Ti(IV) isopropoxide. The nanocrystalline TiO₂ photoelectrodes were prepared by depositing the paste onto transparent conducting FTO glass (or IBE, 7 Ω /square) according to the well-known “scotch tape” method. The thin films were allowed to dry at room temperature for 20 min and finally fired at 450 $^\circ\text{C}$ for 40 min. The still hot electrodes were immersed in the dye solution and kept at 80 $^\circ\text{C}$ for 5 h, after which the absorption was deemed complete. The efficiency of absorption was evaluated by UV–vis spectroscopy: photoelectrodes characterized by an optical density ≥ 1 at the MLCT maximum of the sensitizer were commonly obtained. Dye solutions were prepared by dissolving a small amount of the Ru(II) complex in anhydrous ethanol (ca. 4 mg in 10 mL of solvent). The solutions were sonicated and filtered to remove suspended undissolved dye.

Counter Electrodes Preparation. Platinum-coated counter electrodes were obtained by spraying a 5×10^{-3} M H₂PtCl₆ (Fluka) solution in isopropanol on the well cleaned surface of an FTO glass. This procedure was repeated 5–10 times to obtain an homogeneous distribution of H₂PtCl₆ droplets. The electrodes were dried under a gentle air flow and treated in an oven at 380 $^\circ\text{C}$ for 15 min, obtaining the formation of stable platinum clusters.

Photoelectrochemical Cell Assembly.²² Parafilm sealed cells were built by pressing the sensitized photoanode against a counter electrode equipped with a parafilm frame used to confine the liquid electrolyte inside the cell. The thickness of liquid layer corresponded roughly to the thickness of the frame borders (≈ 120 μm). In this configuration, the cell was stable toward solvent evaporation and leaking for several days even using volatile solvents like acetonitrile. In both cases, metallic clamps were used to firmly hold the two electrodes together.

The mediators $\text{Fe}(\text{DMB})_3^{2+}$ and $\text{Co}(\text{DTB})_3^{2+}$ were prepared according to published procedures.^{22,23}



Chemical reagents and solvents were commercially available and used as such except ligands **L1**, **L2**, which were prepared according to our previous works.^{20,24}

Transient spectroscopy experiments on the dyed TiO₂ photoanodes were carried out by using a previously described transient absorption apparatus.²⁵ The 532 nm laser radiation was defocused with a plano-concave lens to obtain pulse energies of the order of 14 mJ/cm². To obtain a satisfactory S/N ratio, we averaged oscillographic traces over 10 laser shots. No sample degradation was observed over several laser shots.

Preparation of Complexes. $[\text{Ru}(\text{pyrrbpy})_2(\text{dcbpy})](\text{PF}_6)_2$ (**1**) was obtained in 60% yield from procedure reported in ref.²⁰ ¹H NMR (DMSO-*d*₆): δH (ppm) 9.18 (brs, 2H), 9.11 (d, $J = 8$ Hz, 2H), 8.97 (m, 2H), 8.73–8.88 (m, 2H), 8.16–8.26 (m, 2H), 7.71–8.01 (m, 10H), 7.47–7.67 (m, 6H), 6.46 (m, 4H). MS (ES): $m/z = 394.0710$ [$\text{M} - 2\text{PF}_6$]²⁺. UV–vis (CH₃CN), λ_{max} (ϵ) = 472 nm (19000 M⁻¹ cm⁻¹) for the MLCT band.

$[\text{Ru}(\text{pyrrbpy})_2(\text{dcbpy})](\text{PF}_6)_2$ (**2**) was obtained in 70% yield from procedure reported in ref. 20. ¹H NMR (DMF-*d*₇): δH (ppm) 9.87 (brs, 2H), 9.40 (m, 4H), 8.61 (d, $J = 5$ Hz, 2H), 8.39 (d, 6 Hz, 2H), 8.18 (m, 2H), 8.13 (d, $J = 6$ Hz, 2H), 8.07 (m, 8H), 6.69 (m, 8H). MS (ES): $m/z = 1063.1968$ [$\text{M} - \text{PF}_6$]⁺, 459.1146 [$\text{M} - 2\text{PF}_6$]²⁺. UV–vis (CH₃CN): λ_{max} (ϵ) = 483 nm (21000 M⁻¹ cm⁻¹) for the MLCT band.

Preparation of complex *fac*-**4**.²⁶ Ligand **L**³ (53.1 mg, 0.19 mmol), RuCl₃·3H₂O (15.69 mg, 0.06 mmol), and two drops of *N*-ethylmorpholine were suspended in ethyleneglycol (5 mL) and the mixture was refluxed (196 $^\circ\text{C}$) for 14 h or alternatively irradiated in the CEM discover microwave oven (250 W, 200 $^\circ\text{C}$, 4 min). Once cold, the orange solution was poured into a saturated aqueous solution of KPF₆ (25 mL) and left in the fridge (4 $^\circ\text{C}$) for 5–6 h. The red solid formed was filtered and washed with water, toluene, and diethyl ether. The solid obtained was dissolved in the minimum amount of acetonitrile, poured into water (25 mL), and left precipitating into the fridge. After filtration and washing (water, toluene, diethyl ether), **3** was obtained as a dark red solid. Yield: 65 mg (82%). ¹H NMR (400 MHz, acetone-*d*₆) δ (ppm): 9.40 (brs, 1H); 9.25 (brs, 1H); 8.46 (*dd*, $J = 10.4$ and 6.0 Hz, 1H); 8.16 (*dd*, $J = 12.4$ and 6.4 Hz, 1H); 8.02 (*dd*, $J = 5.8$ and 1.5 Hz, 1H); 7.82 (*d*, $J = 6.0$ and 1.6 Hz, 1H); 7.72 (*s*, 2H); 6.47 (*s*, 2H); 4.48 (brs, 2H); 4.12 (brs, 1H); 3.89 (brs, 2H). Mass spectrometry (ESI): 1174.0 [$\text{M} - \text{PF}_6$]⁺; 514.6 [$\text{M} - 2\text{PF}_6$]²⁺.

Complex **3** (13.19 mg, 0.01 mmol) was dissolved in THF (5 mL) and the mixture was sonicated until complete dissolution.

(24) Martineau, D.; Gros, P. C.; Beley, M.; Fort, Y. *Eur. J. Inorg. Chem.* **2004**, 3984–3986.

(25) Cazzanti, S.; Caramori, S.; Argazzi, R.; Elliott, C. M.; Bignozzi, C. *A. J. Am. Chem. Soc.* **2006**, *128*, 9996–9997.

(26) Grabulosa, A.; Beley, M.; Gros, P. C. *Eur. J. Inorg. Chem.* **2008**, 2008, 1747–1751.

(22) Sapp, S. A.; Elliott, C. M.; Contado, C.; Caramori, S.; Bignozzi, C. *A. J. Am. Chem. Soc.* **2002**, *124*, 11215–11222.

(23) Cazzanti, S.; Caramori, S.; Argazzi, R.; Elliott, C. M.; Bignozzi, C. *A. J. Am. Chem. Soc.* **2006**, *128*, 9996–9997.

Table 1. Photophysical and Electrochemical Properties of Complexes **1**, **2**, and **4**

dyes	$\lambda_{\text{abs-max}}$ (nm) ^a	ϵ ($\times 10^3$) $\text{M}^{-1}\text{cm}^{-1}$)	$\lambda_{\text{em-max}}$ (nm) ^b	ϕ_{em} (%)	τ (ns)	$E_{1/2}\text{Ru}^{\text{III}}/\text{Ru}^{\text{II}}$ (ΔE_{p}) (V/SCE) ^c	ligand processes (V/SCE) ^d	$E^*_{1/2}\text{Ru}^{\text{III}}/\text{Ru}^{\text{II}*}$ (V/SCE) ^e	E^{00} (eV) ^f
Ru(L1) ₃ ²⁺	465	8.6	630	0.022	635	1.16 (90)	−1.21 (rev.)	−0.93	2.09
Ru(L2) ₃ ²⁺	480	22.2	650	0.044	357	1.12 (90)	−1.20 (rev.)	−0.91	2.03
1	472	19.0	705	0.019	435	1.19 (100)	−1.35 (irrev.)	−0.78	1.97
2	483	21.0	730	0.010	224	1.14 (100)	−1.18 (irrev.)	−0.81	1.95
4	474	24.7	650	0.039	419	0.86 (120)	−0.84 (irrev.)	−1.33	2.19

^a Measured in CH₃CN at 25 °C. ^b $\lambda_{\text{excit}} = 475$ nm, OD < 0.05 in the absence of O₂. ^c First oxidation potential standardized with Fc⁺/Fc as internal standard and converted into SCE scale by adding 0.33 V ($E_{1/2}\text{Fc}^+/\text{Fc}$), recorded at 100 mV/s using LiClO₄ as supporting electrolyte. ^d First reduction potential. In case of reversibility, the value stands for $E_{1/2}(\text{L}/\text{L}^-)$. If irreversibility, the value stands for $E_{\text{pc}}(\text{L}/\text{L}^-)$. ^e First oxidation potential at excited state. ^f Energy gap between vibrational levels ($\nu=0$) at the ground and excited state. Determined according to Adamson and Fleischer²⁹ by taking the wavelength ($\lambda_{0.05}$) corresponding to 5% of the maximum intensity of the emission spectrum recorded at 298 K ($E^{\text{00}} = 1240/\lambda_{0.05}$).

A solution of NBu₄OH in methanol (0.2 mL of a 0.1 M solution) was then added, a precipitate formed instantaneously and the suspension was stirred for 1 h at room temperature. Water (5 mL) was then added, dissolving the precipitate. THF was then evaporated under reduced pressure and the pH of the aqueous phase was adjusted to 3 using glacial acetic acid. The formed precipitate was then left in a fridge for 5–6 h. The red solid was then collected by filtration and washed with water and diethylether and dried overnight under reduced pressure, yielding *fac*-**4** as a red solid (9.30 mg, 78%) in pure form. ¹H NMR (400 MHz, DMSO-*d*₆) δ (ppm): 9.35 (brs, 1H); 9.09 (brs, 1H); 7.93 (s, 2H); 7.60–7.80 (m, 4H); 6.42 (s, 2H). Mass spectrometry (ESI): 896.1 [M–2PF₆–H]⁺. C₄₅H₃₃N₉O₆P₂F₁₂Ru₁·2H₂O (1222.85) Calcd: C, 44.19; H, 3.05; N, 10.31. Found: C, 43.88; H, 2.79; N, 10.62. UV–vis (CH₃CN): $\lambda_{\text{max}}(\epsilon) = 478$ nm (24700 M^{−1} cm^{−1}) for the MLCT band.

Results and Discussion

Complexes **1** and **2**, needed for comparison purposes, were prepared following our previous works²⁴ by first reacting respectively **L1** and **L2** (2 equiv) with RuCl₃·*x*H₂O under microwave irradiation, coordination with dcby in refluxing acetic acid, and separation on a Sephadex LH20 column (Scheme 1).

Complex **4** was prepared by first reacting **L3**²⁶ (3 equiv) with RuCl₃·*x*H₂O in ethylene glycol under microwave irradiation. This step resulted in the transesterified complex **3** (Scheme 1). Several conditions screening revealed that only this procedure gave the target product,²⁷ and additionally induced a control of the complex stereochemistry toward *fac*-**3** isomer which the symmetry was revealed by NMR spectroscopy as shown in our recent paper.²⁶ The stereoselectivity could arise from a thermodynamically favored arrangement placing the more electron-withdrawing pyridine ring of a ligand *trans* to the more electron-releasing one of the other according to the so-called *trans*-influence.²⁸ Organizational effects by ethylene glycol groups were also suspected to be involved in the stereospecific process. **3** was finally saponified under mild conditions, yielding **4**, which was obtained as a red solid in 78% yield.

Complex **4** was then subjected to a set of photophysical and electrochemical analyses which were compared with those of **1** and **2**. The data concerning homoleptic complexes²⁴ Ru(**L1**)₃²⁺ and Ru(**L2**)₃²⁺ were added to evaluate the effect of the carboxylic group. The results are summarized in Table 1.

(27) All other conditions tried such as other solvents and thermal heating led to untractable mixtures or incomplete incorporation of the ligands.

(28) Appleton, T. J.; Clark, H. C.; Manzer, L. E. *Coord. Chem. Rev.* **1972**, *10*, 335.

UV–Vis Spectroscopy. In the UV region, the ligand-centered transitions appeared as intense bands (Figure 1). The band near 300 nm was attributed to a π – π^* transition localized mostly on bipyridine. Near 250 nm were found π – π^* transitions localized on pyrrole. Interestingly, dye **4** exhibited higher absorption than dye **1** at 250 nm, in agreement with the presence of an additional pyrrole moiety in the complex. A slight ipsochromic effect was observed compared to dyes **1** and **2** because of the presence of both the carboxylic group and pyrrole on the ligand. (Figure 1).

In the visible part of the spectrum, all the complexes exhibited MLCT absorption bands with absorption maxima around 475 nm. **4** displayed the highest molar extinction coefficient ($\epsilon = 24700$ M^{−1} cm^{−1}), whereas 19000 and 21000 M^{−1} cm^{−1} were measured for **1** and **2**, respectively. This coefficient was even higher than those of Ru(**L2**)₃²⁺. This could be explained by the donor–acceptor character of the dissymmetrical ligand leading to an increase of the electric dipole moment associated with the charge-transfer transition.

Like **1** and **2**, **4** was found emissive in fluid solution upon excitation into the MLCT band (475 nm). However the emission maximum was found at 650 nm instead of higher values for **1** and **2**. This blue shift came with an increase of excited-state lifetime ($\tau = 419$ ns) and quantum yield ($\phi_{\text{em}} = 0.039\%$). These values were similar to those obtained for the homoleptic complex Ru(**L2**)₃²⁺.

Transient Absorption. Transient absorption spectra of **4** in ethanol solution have been performed at various time delays using a laser excitation at 532 nm (0.14 mJ/pulse). As shown in Figure 2, the transient absorption features are consistent with a long-lived triplet MLCT excited state, showing an intense absorption in the UV region and a broad absorption at lower wavelengths up to the IR range, arising from electronic transitions localized on the reduced ligand. The excited/ground state isosbestic point was observed at 422 nm, whereas the maximum absorption bleach was centered at 475 nm, in good agreement with the MLCT absorption λ_{max} .

Electrochemistry. All the oxidation potentials of the Ru^{III}/Ru^{II} couple were found reversible. **4** was oxidized at lower potential ($E_{1/2}\text{Ru}^{\text{III}}/\text{Ru}^{\text{II}} = 0.86$ V/SCE) than the heteroleptic dyes **1** and **2**. This signed an increase of the HOMO energetic level in the homoleptic complex with the dissymmetrical ligand. Because similar λ_{max} absorption values were obtained with all complexes for the MLCT transition, the low oxidation potential for **4** was probably due to an electrochemically induced process.

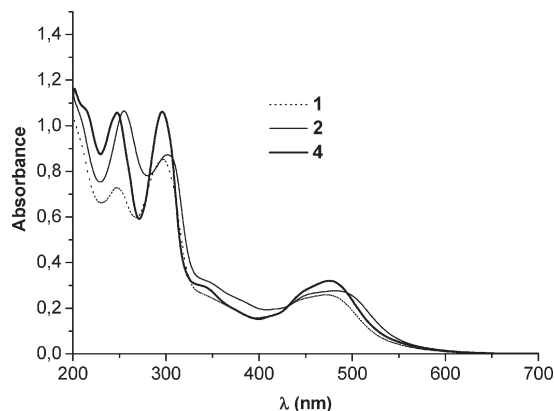


Figure 1. UV-vis spectra of dyes **1**, **2**, and **4** in acetonitrile.

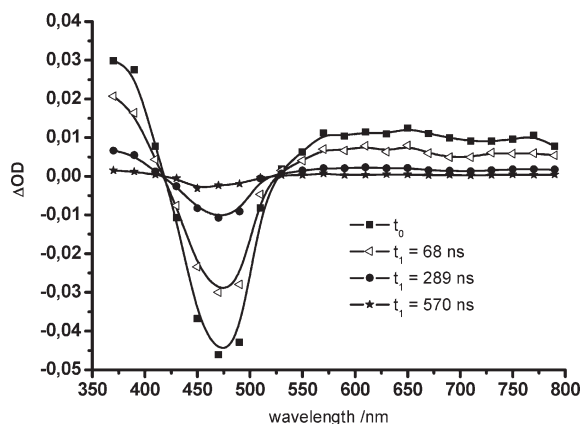


Figure 2. Transient absorption spectra of **4** in ethanol.

Indeed, only one oxidation wave was observed indicating a concomitant oxidation of both the pyrrole ring and Ru^{III}/Ru^{II} couple. Therefore, the radical cation of pyrrole could be stabilized by intraligand delocalization through the pyridine bearing the carboxylic group, thus increasing electron density on the metal and consequently lowering the oxidation potential.

Such a stabilization of pyrrole radical cation was in agreement with our unsuccessful attempts to electropolymerize **4** at the Pt electrode by repeated scans in contrast with **1** and **2**. The modification of the HOMO energy level appears only for the oxidized form of **4**, consequently, the electrochemical and spectroscopic orbitals are different and cannot be compared.

Like heteroleptic complexes **1** and **2**, and in contrast with homoleptic complexes Ru(L**1**)₃²⁺ and Ru(L)₃²⁺, **4** led to irreversible L/L⁺ processes and reduction was observed at a higher potential (−0.84 V). The excited-state oxidation potential $E^*_{1/2\text{ox}}$ ($E^*_{1/2\text{ox}} = [E_{1/2\text{Ru}^{\text{III}}/\text{Ru}^{\text{II}} - E^{00}]$) for dye **4** was found at −1.33 V/SCE, indicating an adequate excited state reducing power to allow for the electron injection because the TiO₂ flat band potential is typically near −0.7 V/SCE.³⁰

These first measurements revealed the good visible light harvesting ability of dye **4**, which was comparable with

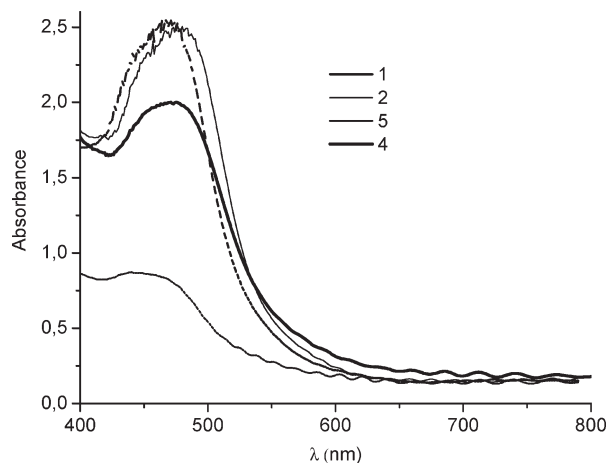


Figure 3. Overlay absorption spectra of TiO₂ photoanodes modified with dyes **1**, **2**, **4**, and **5**.

those of heteroleptic complexes **1** and **2**. Thus we turned to the investigation of the sensitizing experiments with this dye and evaluation of its performance in a photo-voltaic device.

IPCE Measurements. The complexes **1**, **2**, and **4** were chemisorbed on TiO₂ films and the semiconductor sensitization controlled by UV-vis spectroscopy (Figure 3). The spectra were compared to those of known reference dye [Ru(dcbpy)₃]²⁺ (**5**)³¹ to evaluate the effect of pyrrole in **4**.

TiO₂ electrode coated with **4** exhibited a maximum absorbance slightly lower than those of heteroleptic complexes **1** and **2** despite a better molar extinction coefficient in solution (Table 1). The absorbance and absorption range were far better than those of **5**, clearly indicating the effect of the electron-donor pyrrole on the increase of dipolar moment. The absorption range was comparable with those of the heteroleptic complexes.

All the absorption maxima of chemisorbed complexes were about 10 nm lower than in solution. This blue shift can be explained by a weakening of the electronic charge on the dye by the electron-withdrawing TiO₂. Another factor is also the electron delocalization through TiO₂–dye interface titanates inducing the HOMO level stabilization.

The promising absorption profile of **4** was found of particular interest to investigate DSC assembly and IPCE measurements (Figure 4). The DSC was built following reported methods²² and photoelectrochemical experiments were performed using various electron transfer mediators in the electrolyte including the most popular I[−]/I₃[−] couple (platinum cathode) and Co^{II}-based mediators^{22,23} (gold cathode) including also various Fe-based comediators expected to induce faster regeneration of Ru^{II} state.

The best result was recorded using a mixture of [Fe(DMB)₃]²⁺ (dmbpy = 4,4'-dimethyl-bipyridine) and [Co(DTB)₃]²⁺ (dtbbpy = 4,4'-diterbutyl-bipyridine) as mediator. Under these conditions **4** attained a good 65% IPCE value within the maximum absorption range. All other mediators such as I[−]/I₃[−], [Co(DTB)₃]²⁺ alone or

(29) Adamson, A. W.; Fleischauer, P. D. *Concepts Inorg. Photochem.* **1975**, 381.

(30) Gratzel, M. *Inorg. Chem.* **2005**, *44*, 6841–6851.

(31) Vlachopoulos, N.; Liska, P.; Augustynski, J.; Grätzel, M. *J. Am. Chem. Soc.* **1998**, *110*, 1216.

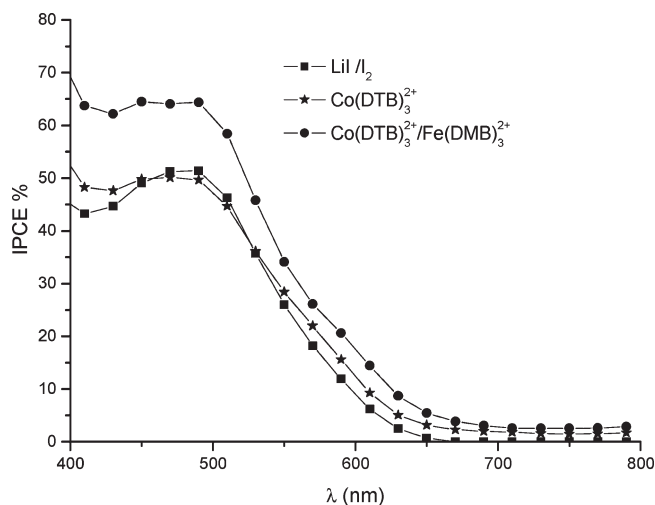


Figure 4. Photoaction spectra of **4** with various mediators I^- (0.15 M), $Co(DTB)_3^{2+}$ (0.15 M) and $Co(DTB)_3^{2+}/Fe(DMB)_3^{2+}$ (0.015 M) in acetonitrile. $LiClO_4$ (0.5 M) was present in every electrolyte solution.

associated with Fe complexes containing other bipyridine ligands than DMB led to lower performance (near 50% IPCE).

These mediator effects on the IPCE could not be explained on a simple thermodynamic basis. Indeed, the oxidation potentials were found at 0.86, 0.4, and 0.2 V/SCE for **4**, I^-/I_3^- and Co^{II}/Co^{III} respectively. Thus both the mediators should regenerate the Ru^{II} state in **4** with the same efficiency.

In order to get a deeper insight into this mediator effect, transient absorption spectroscopy was used to investigate the interaction between the dye and the electron mediators (Figure 5). From these experiments, it appeared that the regeneration of **4** was very fast, within a few nanoseconds, by iodide (7 ns). The regeneration by $[Co(DTB)_3]^{2+}$ was found to be much slower (114 ns), but despite that, the IPCE generated in the presence of the iodide/iodine electrolyte. The kinetic effect obtained by addition of a fast couple like $[Fe(DMB)_3]^{2+}$ was clearly evidenced by a half regeneration time (55 ns). While the accelerating effect of $[Fe(DMB)_3]^{2+}$ was in agreement with the increased performance (based on IPCE) compared to $[Co(DTB)_3]^{2+}$ alone, the lower performance with the fastest iodide mediator remained unclear with regard to the dye regeneration kinetics.

Such a discrepancy between fast regeneration kinetics and performance could be explained by a fast recombination of photoinjected electrons with the oxidized mediator in case of the I^-/I_3^- couple. This process could be favored by mediator oxidized form adsorbed at the

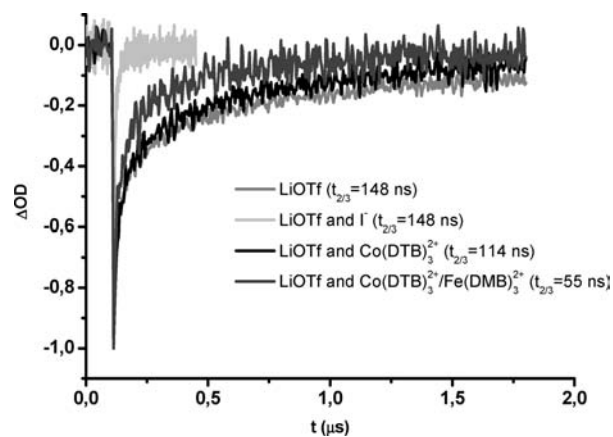


Figure 5. Transient absorption spectra of dye-sensitized TiO_2 with **4** in the presence of $LiOTf$ (0.5 M), I^- (0.15 M), $Co(DTB)_3^{2+}$ (0.15 M), and $Co(DTB)_3^{2+}/Fe(DMB)_3^{2+}$ (0.015 M) in acetonitrile ($\lambda_{exc} = 532$ nm, $\lambda_{obs} = 500$ nm; power intensity = 14 mJ/pulse).

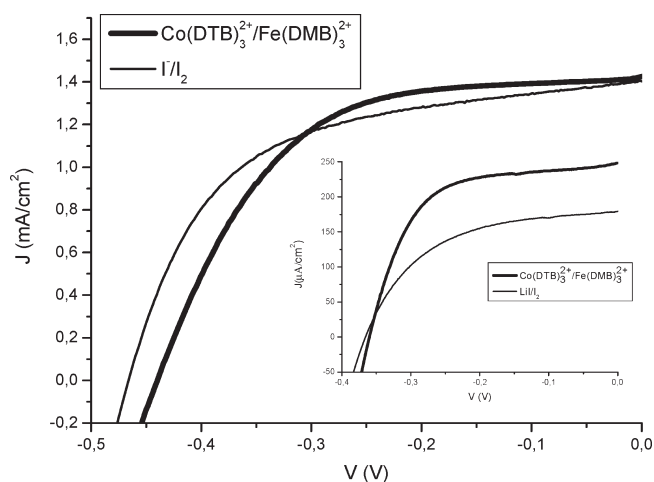


Figure 6. $J-V$ curve recorded under AM 1.5 G irradiation (16 mW/cm²) in the presence of $Fe(DMB)_3^{2+}/Co(DTB)_3^{2+}$ and I^-/I_2 mediators. Inset: same as in Figure 6 under 480 nm monochromatic irradiation (1 mW/cm²).

semiconductor surface.^{32,33} Additionally, based on recent works,^{34–36} the iodide mediator could also chemically interact with the dye, leading to stabilization of the first reduction product of I_2 (namely I_2^-). The consequence is a slowing down of its dismutation into I_3^- and I^- in the bulk solution and thus its efficient capture by the photoinjected electrons. This surface and dye interactions are unlikely with the bulky $[Co(DTB)_3]^{2+}/[Fe(DMB)_3]^{2+}$, which despite a lower regeneration kinetic finally led to slower recombination rates and better overall performance.

To gain additional information about the electron mediator effects in association with **4**, we recorded $J-V$ curves under relatively low light intensities to avoid the set in of mass transport limitations, which are expected in the case of bulky cobalt complexes and may conceal kinetic effects intrinsic to the electron mediator nature. From Figure 6 and Table 2, it is evident that the $Fe(II)/Co(II)$ mediator generally produced higher J_{sc} and better fill factors, whereas the V_{oc} was slightly lower than that generated by the iodide/iodine electrolyte.

However, it must be recalled that the cell V_{oc} is given by $E_F(TiO_2) - E_{1/2}$, where E_F is the Fermi level of TiO_2 and

(32) Huang, S. Y.; Schlichthorl, G.; Nozik, A. J.; Gratzel, M.; Frank, A. J. *J. Phys. Chem. B* **1997**, *101*, 2576–2582.

(33) Gregg, B. A.; Pichot, F.; Ferrere, S.; Fields, C. L. *J. Phys. Chem. B* **2001**, *105*, 1422–1429.

(34) O'Regan, B. C.; Lopez-Duarte, I.; Martinez-Diaz, M. V.; Forneli, A.; Albero, J.; Morandeira, A.; Palomares, E.; Torres, T.; Durrant, J. R. *J. Am. Chem. Soc.* **2008**, *130*, 2906–2907.

(35) O'Regan, B. C.; Walley, K.; Juozapavicius, M.; Anderson, A.; Matar, F.; Ghaddar, T.; Zakeeruddin, S. M.; Klein, C. d.; Durrant, J. R. *J. Am. Chem. Soc.* **2009**, *131*, 3541–3548.

(36) Gardner, J. M.; Giacomucci, J. M.; Meyer, G. J. *J. Am. Chem. Soc.* **2008**, *130*, 17252–17253.

Table 2. Photovoltaic Device Parameters Obtained in the Presence of Fe(II)/Co(II) and I^-/I_3^- Mediators

electron mediator	incident irradiance (mW/cm ²)	J_{sc} (mA/cm ²)	V_{oc} (V)	FF	η (%)
Fe(DMB) ₃ ²⁺ /Co(DTB) ₃ ²⁺	16.5 ^a	1.42 (0.54)	0.44 (0.36)	0.56 (0.56)	2.14 (0.67)
Fe(DMB) ₃ ²⁺ /Co(DTB) ₃ ²⁺	1 ^b	0.248 (0.18)	0.360 (0.26)	0.61 (0.48)	5.4 (2.25)
LiI/I ₂	16.5 ^a	1.40 (2.1)	0.46 (0.48)	0.56 (0.48)	2.2 (2.92)
LiI/I ₂	1 ^b	0.180 (0.166)	0.365 (0.33)	0.52 (0.43)	3.4 (2.33)

^a AM 1.5G irradiation. ^b monochromatic 480 nm irradiation. In parentheses, values measured for N719 under the same irradiating conditions.

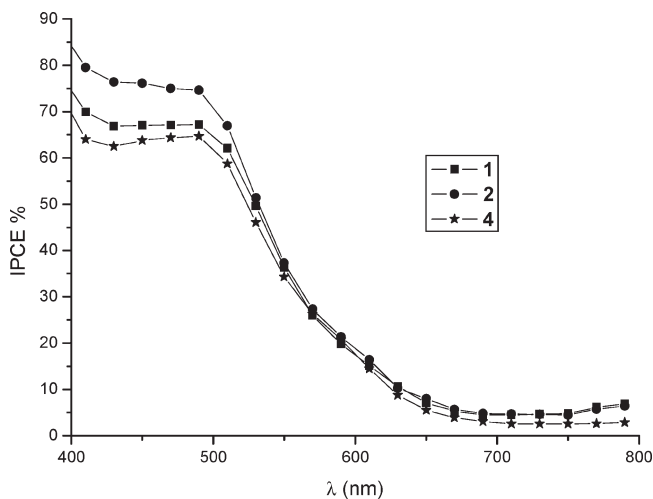


Figure 7. Comparison of the photoaction spectra of **1**, **2**, and **4** with Co(DTB)₃²⁺ (0.15M)/Fe(DMB)₃²⁺ (0.015 M) in acetonitrile. LiClO₄ (0.5 M) was present in every electrolyte solution.

$E_{1/2}$ is the half wave potential of the redox couple. Because Co(II)/(III) is about 200 mV more negative than I^-/I_3^- , the small difference (20 mV) found between the V_{oc} generated by the Fe(II)/Co(II) electrolyte by the iodide/iodine couple can be explained by a negative shift (ca. $-180/-150$ mV) of the Fermi level of the TiO₂ in the presence of the cobalt based mediator. This negative shift is consistent with a higher stationary electronic density in the TiO₂, which indeed is explainable by a decreased recombination rate between photoinjected electrons and accepting electrolyte species. For comparison, the results obtained with **N719**,¹⁷ which is one of the most efficient bipyridine-based dye, have been reported in Table 2. As shown, in contrast with **4**, **N719** led to higher overall efficiencies using I^-/I_3^- than with the Fe(II)/Co(II) mediator. An especially poor yield was obtained under AM 1.5G irradiation (0.67%).

As shown, the overall efficiency of our cell is quite low under AM 1.5 irradiation. However the achievement of record efficiency was not the aim of our paper which was rather focused on the basic photoelectrochemical

characterization of a potentially interesting family of new dyes. Laser spectroscopy used here is a primary tool for understanding the interaction between the dye and new electron mediators; consequently, we usually operate with thin ($5-6 \mu\text{m}$) transparent TiO₂ photoanodes, which are ideally suited for spectroscopic transmission measurements but do not allow for record power conversion efficiency.³⁷ It must be recalled that the efficiency of the cell is critically dependent upon TiO₂ substrate engineering. High efficiency cells are usually obtained with relatively thick ($12-18 \mu\text{m}$) TiO₂ films often equipped with a scattering overlayer, which, for example, nearly double photon absorption in the spectral region where the dye extinction coefficient is low.³⁸

Using the best Fe(DMB)₃²⁺-Co(DTB)₃²⁺ mediator, **4** displayed interesting performances (65%) slightly lower than those previously obtained for bis-heteroleptic dyes **1** and **2** (68 and 75% IPCE, respectively) with a comparable absorption domain (Figure 7).

Conclusion

In summary, we have shown that a homoleptic complex easily accessed from a dissymmetrical bipyridine bearing an electron-donor pyrrole and an accepting-anchoring carboxylic moiety can be used successfully as sensitizer in DSC. The choice of the mediator used for regeneration of the Ru^{II} state was found critical. The best results were obtained with a combination of Co(DTB)₃²⁺ and Fe(DMB)₃²⁺, which offered an adequate balance between regeneration of the dye and back recombination with photoinjected electrons in TiO₂. Under these conditions, the overall yield of the DSC was much better than those of **N719** under AM 1.5 G irradiation. These first results are promising and work is progressing to optimize the performance of this new family of dyes.

Acknowledgment. The authors thank the CNRS, the Région Lorraine, and Nancy University for a grant to A.G. The technical assistance of Mr. Sandro Fracasso is also gratefully acknowledged.

(37) Koops, S. E.; O'Regan, B. C.; Barnes, P. R. F.; Durrant, J. R. *J. Am. Chem. Soc.* **2009**, *131*, 4808–4818.

(38) Nazeeruddin, M. K.; De Angelis, F.; Fantacci, S.; Selloni, A.; Viscardi, G.; Liska, P.; Ito, S.; Takeru, B.; Gratzel, M. *J. Am. Chem. Soc.* **2005**, *127*, 16835–16847.